



# Cognitive Deficits and Alzheimer's Disease-Like Pathologies in the Aged Chinese Tree Shrew

Hongli Li<sup>1,2</sup> · Bo-Lin Xiang<sup>1,2</sup> · Xiao Li<sup>1,2</sup> · Cong Li<sup>2,3</sup> · Yu Li<sup>1,2</sup> · Ying Miao<sup>1,4</sup> · Guo-Lan Ma<sup>5</sup> · Yu-Hua Ma<sup>6</sup> · Jia-Qi Chen<sup>6</sup> · Qing-Yu Zhang<sup>6</sup> · Long-Bao Lv<sup>6</sup> · Ping Zheng<sup>3,6,7</sup> · Rui Bi<sup>1,2</sup> · Yong-Gang Yao<sup>1,2,6,7</sup>

Received: 11 May 2023 / Accepted: 12 September 2023 / Published online: 9 October 2023  
© The Author(s), under exclusive licence to Springer Science+Business Media, LLC, part of Springer Nature 2023

## Abstract

Alzheimer's disease (AD) is the most common chronic progressive neurodegenerative disease in the elderly. It has an increasing prevalence and a growing health burden. One of the limitations in studying AD is the lack of animal models that show features of Alzheimer's pathogenesis. The tree shrew has a much closer genetic affinity to primates than to rodents and has great potential to be used for research into aging and AD. In this study, we aimed to investigate whether tree shrews naturally develop cognitive impairment and major AD-like pathologies with increasing age. Pole-board and novel object recognition tests were used to assess the cognitive performance of adult (about 1 year old) and aged (6 years old or older) tree shrews. The main AD-like pathologies were assessed by Western blotting, immunohistochemical staining, immunofluorescence staining, and Nissl staining. Our results showed that the aged tree shrews developed an impaired cognitive performance compared to the adult tree shrews. Moreover, the aged tree shrews exhibited several age-related phenotypes that are associated with AD, including increased levels of amyloid- $\beta$  (A $\beta$ ) accumulation and phosphorylated tau protein, synaptic and neuronal loss, and reactive gliosis in the cortex and the hippocampal tissues. Our study provides further evidence that the tree shrew is a promising model for the study of aging and AD.

**Keywords** Alzheimer's disease · Tree shrew · Amyloid accumulation · Tau phosphorylation · Gliosis · Cognitive deficits

## Introduction

Alzheimer's disease (AD) is the most common chronic progressive neurodegenerative disease in the elderly. The disease has an increasing prevalence and a worsening

---

Hongli Li and Bo-Lin Xiang contributed equally to this work

✉ Rui Bi  
birui@mail.kiz.ac.cn

✉ Yong-Gang Yao  
yaoyg@mail.kiz.ac.cn

<sup>1</sup> Key Laboratory of Animal Models and Human Disease Mechanisms of the Chinese Academy of Sciences & Yunnan Province, and KIZ-CUHK Joint Laboratory of Bioresources and Molecular Research in Common Diseases, Kunming Institute of Zoology, Kunming 650204, Yunnan, China

<sup>2</sup> Kunming College of Life Science, University of Chinese Academy of Sciences, Kunming 650204, Yunnan, China

<sup>3</sup> State Key Laboratory of Genetic Resources and Evolution, Kunming Institute of Zoology, Chinese Academy of Sciences, Kunming 650204, Yunnan, China

<sup>4</sup> Hefei National Laboratory for Physical Science at the Microscale, School of Life Science, Division of Life Science and Medicine, University of Science and Technology of China, Hefei 230026, Anhui, China

<sup>5</sup> Kunming Biological Diversity Regional Center of Large Apparatus and Equipments, Public Technology Service Center, Kunming Institute of Zoology, Chinese Academy of Sciences, Kunming 650204, Yunnan, China

<sup>6</sup> National Research Facility for Phenotypic & Genetic Analysis of Model Animals (Primate Facility), National Resource Center for Non-Human Primates, Kunming Institute of Zoology, Chinese Academy of Sciences, Kunming 650107, China

<sup>7</sup> Center for Excellence in Animal Evolution and Genetics, Chinese Academy of Sciences, Kunming 650204, Yunnan, China

healthcare burden [1–3]. Although the exact pathophysiology of AD remains controversial, growing evidence has shown that AD is characterized by cognitive impairment, brain atrophy, extracellular plaques formed by aggregated amyloid- $\beta$  (A $\beta$ ) deposits, intracellular neurofibrillary tangles (NFTs) composed of hyperphosphorylated microtubule-associated protein tau (MAPT), synaptic degeneration, neuronal loss, and gliosis [1, 2, 4, 5]. The amyloid-related immunotherapeutic antibodies aducanumab, BAN2401, and gantenerumab were reported to reduce AD pathologies including A $\beta$  plaques, phosphorylated tau, neurogranin, and neurofilament light [2, 6]. Although aducanumab and BAN2401 have been approved by the FDA, there are still many controversies on their efficacy [6]. Promising preclinical results have largely failed to translate into effective treatments, and there are still no drugs with validated efficacy that can cure AD patients [7]. There are many researchers working on new therapeutic strategy, which are expected to be beneficial for the treatment of AD in the future [8–13].

Research into treatments for AD has been hindered by the limited availability of animal models in which potential drugs can be tested, and the creation of better animal models may be the best way to make progress [7, 14, 15]. An ideal animal model would promote the understanding of the pathogenesis of AD and the discovery of potential therapeutic targets. Unfortunately, neurofibrillary tangles and A $\beta$  plaques do not occur naturally in inbred mice, possibly because of their relatively short lifespan and the large genetic difference between human and rodents [14–16]. For this reason, Dr. De Strooper has claimed that “the biggest mistake you can make, is to think you can ever have a mouse with AD” [17]. Some researchers have tried to develop animal models that more closely mimic the progression and pathobiology of AD [14, 18–22], or to find new experimental animals that may show some of the features of AD pathogenesis [16, 23–26]. There is no doubt that non-human primates with spontaneous AD-like symptoms and pathological changes in the elderly individuals will provide valuable animal models for AD research [18, 23–25]. However, the use of some animals is limited by factors such as high maintenance costs, low reproductive output, manipulation challenges, and ethics issues [14, 27, 28]. There is clearly an urgent need to generate additional animal models for research into AD.

The Chinese tree shrew (*Tupaia belangeri chinensis*) belongs to the order Scandentia, and is widely distributed in Southeast Asia, South, and Southwest China. It has several features that make it useful as a small laboratory animal. The advantages are a short reproductive cycle (about 6 weeks), a short lifespan (6–8 years), a small body size (100–150 g), and low maintenance costs, when compared to non-human primates [29–31]. Based on comparative

genomic analyses, previous studies have shown that the tree shrew has a much closer genetic affinity to non-human primates than that of rodents [32–34]. For several decades, the tree shrew has been considered as a very useful animal model for studying a variety of human diseases [30, 35–44] and for basic research [37, 38, 45–55].

In our previous studies [16, 34], we have provided direct evidence that the AD pathway genes in the tree shrew have a higher protein sequence identity and more similar expression pattern in brain tissue compared to humans than in the mouse. Notably, the A $\beta_{42}$  peptide sequence of the Chinese tree shrew was completely identical to that of the human, whereas three residues differ between rodents (including rats and mice) and humans [16, 56]. Similarly, the related genes of the NFTs formation pathway in tree shrews showed a high degree of protein sequence identity with human orthologs [16]. Previous studies have also reported an early stage of A $\beta$  accumulation and some A $\beta$  deposits in the brain tissues of aged tree shrews [57, 58], despite potential controversies [16]. The hippocampal tissues from aged tree shrews contained an increased number of activated microglia containing ferritin, increased levels of oxidative stress, and hyperphosphorylation of tau [59]. Moreover, intracerebroventricular injection of A $\beta_{40}$  induced cognitive impairment in adult tree shrews, accompanied by the detection of neurotic plaques, NTFs, and neuronal apoptosis in the hippocampal tissues [60].

In this study, we measured the common pathological features of AD in aged tree shrews. We found abnormal changes, including impaired cognitive performance, and increased levels of A $\beta$  accumulation, phosphorylated tau, synaptic degeneration, neuronal loss, and gliosis in aged animals compared to adult tree shrews. Our results provide further evidence to support the Chinese tree shrew as being a potentially important animal model for the study of AD and aging.

## Materials and Methods

### Animals

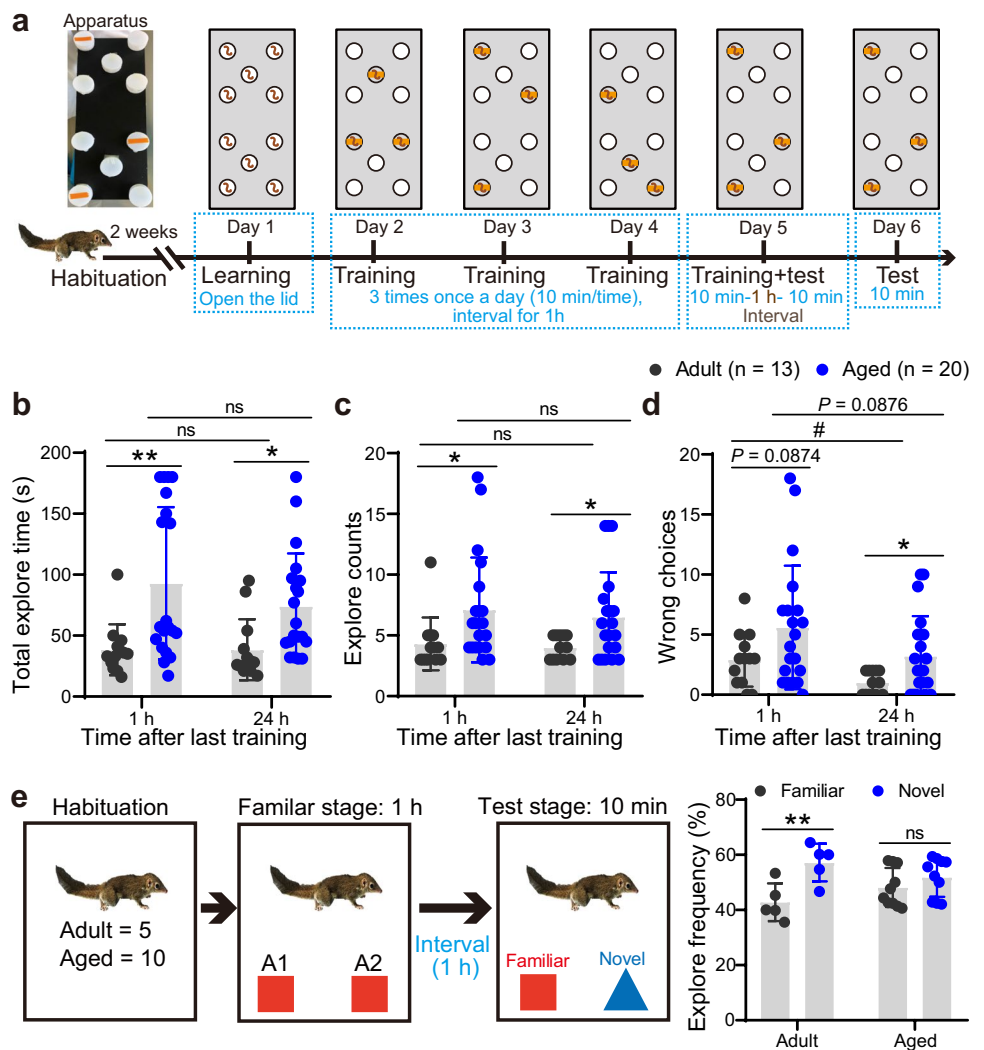
Thirteen adult (about 1 year old) and 24 aged (6 years old, or older) male Chinese tree shrews were randomly chosen from the breeding colonies [61] of the Experimental Animal Center of the Kunming Institute of Zoology, Chinese Academy of Sciences. Animals were of normal weight and behavior and were individually housed in a fully acclimatized facility with access to food twice daily and water ad libitum under a 12-h inverted day/night cycle (lights on at 7:00 a.m. and lights off at 7:00 p.m.). All animal experiments were conducted in compliance with the Animal Ethics Committee of the Kunming Institute of Zoology, Chinese Academy of Science (Approval number: IACUC18027).

### Hole-Board Test

The hole-board test is commonly used to assess cognitive performance in rodents, tree shrews, and non-human primates [36, 62, 63]. We used the procedure as described by Ohl et al. [36], with some modifications, to test the cognitive performance of both the adult ( $n = 13$ ) and the aged ( $n = 20$ ) tree shrews. Briefly, the test apparatus consisted of a black PVC board (105 mm \* 297 mm) containing 10 white holes (diameter 15 mm) staggered in three lines (Fig. 1a). Each hole was covered by a movable white lid made of the same material as the board. The tree shrew has to open the lid in order to find a reward. We recorded the time it took each animal to complete this task and the number of incorrect actions taken. Tree shrews were given a 2-week acclimation period after arriving at the facility. They were fed with apple or yellow mealworms once a day by the experimenter. After acclimation, each tree shrew was given an individual hole-board to avoid potential odor disturbance in the home cage. On day 1

of the test, the tree shrews were allowed to learn how to open the lids to obtain yellow mealworms in randomly selected holes of the hole-board. On the following 3 days of training, the tree shrews were allowed to find three randomly selected holes marked with orange tape containing yellow mealworm in the hole-board (Fig. 1a). We changed the location of the holes labeled with yellow mealworm once a day, so that the animals learned the association between the labels and the food. On day 5, the tree shrews were given a trial of 10 min to find the marked holes, followed by two further tests at 1-h and 24-h intervals with the same marked holes as in the training stage (Fig. 1a). We cleaned the apparatus with ethanol and a paper tissue and filled the holes with fresh yellow mealworms after each trial. During the test, we captured videos until the animals completed the task. The total exploring time, number of explorations, and wrong choices (opened unlabeled holes without mealworm) were calculated by analyzing the videos. The total exploring time was recorded as 180 s if the animal did not open all three baited holes within 3 min.

**Fig. 1** The aged Chinese tree shrews showed cognitive deficits. **a** The apparatus of the modified hole-board test. **b–d** The total exploring time (**b**), exploring counts (**c**), and wrong choices (**d**) of the adult and aged Chinese tree shrews in the tests of 1-h and 24-h intervals after training. Adult tree shrews,  $n = 13$ ; Aged tree shrews,  $n = 20$ . **e** The explore frequency of the novel object recognition test. Adult tree shrews,  $n = 5$ ; aged tree shrews,  $n = 10$ . Data represented as mean  $\pm$  SD. ns, no significant; \* $P < 0.05$ ; \*\* $P < 0.01$  vs adult group; # $P < 0.05$ : Adult-1 h vs adult 24-h group, two-tailed unpaired Student's  $t$  test



## Novel Object Recognition

After the hole-board test, a proportion of tree shrews (adult,  $n = 5$ ; aged,  $n = 10$ ) were given a 2-week familiarization period. Then, the tree shrews were familiarized with the pink square objects A1 and A2 for 10 min in the home cage. After the trial, objects were cleaned with 70% ethanol to avoid any olfactory traces. The familiar object A2 was replaced by a novel blue triangular object after a 1-h interval. We captured a 10-min video and counted the number of explorations between familiar and novel objects, respectively. The number of explorations that a tree shrew interacted with each object during the test was converted into the explore frequency, which was calculated by the number of interactions at novel object / (number of interactions at novel object + number of interactions at familiar object).

## Tissue Collection

At the completion of the behavioral tests, the tree shrews (adult,  $n = 5$ ; aged,  $n = 5$ ) were intramuscularly anesthetized with both ketamine (50 mg/kg) and pentobarbital (60 mg/kg) and intracardially perfused with phosphate-buffered saline (PBS). The brain was quickly and carefully removed and immediately dissected into two halves along the midline on the ice. One half was fixed with 4% paraformaldehyde in PBS for histopathological staining. The prefrontal cortex and hippocampus tissues carefully isolated from another half of the brain were snap-frozen in liquid nitrogen and stored at  $-80\text{ }^{\circ}\text{C}$  for biochemical assays.

## Histopathological Staining

Fixed brain tissue was dehydrated and embedded in paraffin, then sectioned coronally at 8- $\mu\text{m}$  thickness. For frozen section, the tissue was soaked in a 30% sucrose solution and preserved at  $4\text{ }^{\circ}\text{C}$  before being sectioned at 30- $\mu\text{m}$  thickness with a cryostat microtome (RIWARD, Minux@FSB800, Shenzhen, China). For immunohistochemistry or immunofluorescence staining, the slices of hippocampal were collected on slides and stained following our previously described procedure [13]. Briefly, the sections were first blocked with 5% bovine serum albumin (BSA, Beyotime Institute of Biotechnology) and 5% normal goat serum (NGS, Beyotime Institute of Biotechnology) in PBST (0.3% Triton-X-100 in PBS, #P1080, Solarbio) for 2 h, then incubated with the corresponding primary antibodies against  $\text{A}\beta_{17-24}$  (clone: 4G8, 1:500, #800701, Biolegend), phosphor-tau (Thr231, AT180, 1:250, #MN1040, ThermoFisher Scientific), GFAP (1:1000, #GB11096, Servicebio), and AIF1/Iba1 (1:500, #A20844, ABclonal) in antibody-diluted solution (0.3% PBST with 1% BSA and 1% NGS) overnight at  $4\text{ }^{\circ}\text{C}$ . After washing 3 times with 0.1% PBST, the

immunohistochemical assays were performed using the UltraSensitiveTMSP IHC kit (rabbit, #KIT-9707; mouse, #KIT-9701, Fuzhou Maixin Biotech). The sections were further visualized with the DAB solution (#DAB-1031, Fuzhou Maixin Biotech), followed by a counterstaining with hematoxylin (#G1005-1, Servicebio). The immunofluorescent slides were incubated for 2 h at room temperature with fluorescence-labeled AlexaFluor 488 or 594-conjugated goat anti-mouse or rabbit IgGs (1:500, Jackson ImmunoResearch Laboratories).

For Nissl staining, the paraffin-embedded sections were dewaxed with dimethylbenzene (#G1128, Servicebio), rehydrated through serially diluted concentrations of ethanol (100%, 95%, 90%, 85%, 70%, 50%, respectively), and then were immersed in Nissl working solution (#G1036, Servicebio) at  $37\text{ }^{\circ}\text{C}$  for 20 min. The sections were then washed with deionized water, and dehydrated through different concentrations of ethanol (50%, 70%, 85%, 90%, 95%, 100%, respectively), and hyalinized with dimethylbenzene.

Images were captured using an Olympus BX61 VS microscope (Olympus) or an Olympus FluoView 1000 confocal microscope (Olympus). Matched sections from approximately the same region from at least 4 different animals were used to count the number of cells with clear and strong signals for each staining (GFAP, Iba1, AT180 or 4G8). Colocalization with nuclear and morphological brown staining was considered as consistent for GFAP and Iba1. Cell counts in each adult or aged individual were normalized to the average cell number of the adult group. Differences between the adult and aged groups were measured by using the indicated statistical methods.

## Western Blotting

Prefrontal cortex and hippocampus tissues were homogenized and lysed in lysis buffer (#P10013, Beyotime Institute of Biotechnology) supplemented with protease inhibitor cocktail (#P1008, Beyotime Institute of Biotechnology) on ice, and protein concentration was determined using the BCA protein assay kit (#P0012, Beyotime Institute of Biotechnology). The detailed protocol was described in our previous study [64]. Briefly, 20  $\mu\text{g}$  total protein per sample was denatured in loading buffer at  $95\text{ }^{\circ}\text{C}$  for 10 min and was separated by sodium dodecyl sulfate–polyacrylamide gel electrophoresis (SDS-PAGE) and transferred onto a polyvinylidene difluoride membrane (#L1620177 Rev D, BioRad). The membrane was incubated with respective primary antibodies against  $\text{A}\beta_{40}$  (#12990, Cell Signaling Technology),  $\text{A}\beta_{42}$  (#14974T, Cell Signaling Technology), total-A $\beta$  (#8243S, Cell Signaling Technology), 4G8, phosphor-Tau (Ser202 and Thr205, AT8, #MN1020, ThermoFisher Scientific), AT180, total tau (#46687S, Cell Signaling Technology), NeuN (D4G40, #24307, Cell Signaling Technology), PSD95 (#36233S,

Cell Signaling Technology), and GFAP, AIF1/IBA1, actin (#AF7018, Affinity Biosciences LTD) at 4 °C overnight. After 3 washes with TBST (Tris-buffered saline, #G0001, Servicebio) containing 0.1% Tween 20 (#A600560-0500, Sangon Biotech), the membranes were incubated with the horseradish peroxidase-conjugated secondary antibody: goat anti-mouse (1:10000, #G1214, Servicebio) or goat anti-rabbit (1:10000, #G1213, Servicebio). The signals were visualized with the ECL Western Blot Detection Kit (#WBKLS0500, Mollipore). Actin was used as loading control; each protein level was normalized to actin. The integral optic density of each target protein was evaluated using ImageJ (National Institutes of Health, Bethesda, MD).

## Statistical Analysis

All statistical analyses were performed using GraphPad Prism version 8.0.1 (GraphPad Software, Inc., La Jolla, CA, USA). Differences between the adult and aged tree shrew groups were analyzed using Student's *t* test. All the values are presented as mean  $\pm$  standard deviation (SD). A *P* < 0.05 was considered as statistically significant.

## Results

### Declined Cognition Performance in the Aged Tree Shrews

To investigate whether there is a difference in recognition performance during aging of tree shrews, we performed the hole-board and novel object recognition tests to both adult and aged tree shrews. The hole-board test involves memory training with food rewards. Reference memory is defined as an animal not visiting the unlabeled holes, while revisiting a labeled hole within a session is a working memory error [65]. The apparatus and experimental design of the hole-board test were modified from Ohl et al. [45] (Fig. 1a). In the hole-board test at both 1 h and 24 h post-training, mean exploration times were less than 50 s in the adult group, but were significantly increased in the aged group (Fig. 1b). Aged tree shrews explored more counts to find a reward as compared to the adult tree shrews in both the 1 h and 24 h post-training (Fig. 1c). The aged tree shrews also had a significantly higher number of wrong choices than the adult animals (Fig. 1d), suggesting a diminished working memory in the aged individuals. There were no obvious changes in the total explore time and the number of explorations of the same group at different time intervals (Fig. 1b and c). Intriguingly, the number of wrong choices in both the adult group and the aged group was substantially fewer at 24-h than at 1-h interval, and the exact reason for this observation remained unknown (Fig. 1d). Consistent with previous results that the working memory of tree

shrews was significantly impaired by aging [66], our results also suggested that aged tree shrews had attenuated memory performance compared to the adult tree shrews.

The novel object test also measures memory performance. Animals tend to interact more with a novel object than with a familiar one. Object recognition is assessed by the frequency or time spent exploring the object [67]. We performed the novel object recognition test following the previously described procedure with some modifications [68] (Fig. 1e). Consistent with previous studies [68, 69], the adult tree shrews exhibited a robust preference for the novel object compared to the familiar object, but there was no exploration preference for the novel object in the aged tree shrews (Fig. 1e), indicating that the aged tree shrews may lose their curiosity for novel objects and have attenuated memory performance.

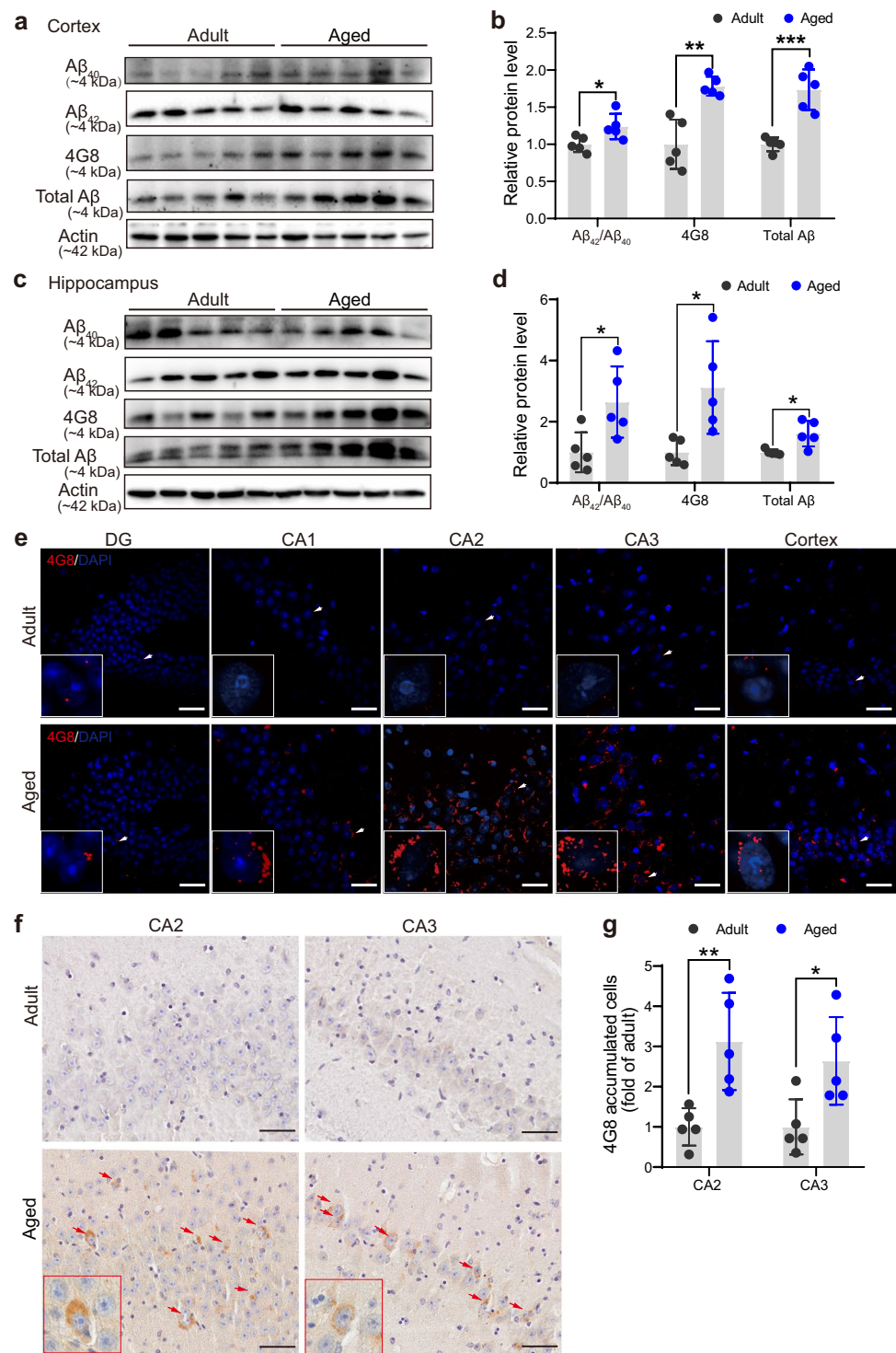
### Increased A $\beta$ Accumulation in the Cortex and Hippocampus Tissues of the Aged Tree Shrews

The A $\beta$  plaque is one of the key pathological features of AD [1, 2, 4]. We investigated whether typical plaques were visible in the brain tissue of aged tree shrews, as previous studies have given inconclusive results [16, 57, 58]. In the present study, the aged tree shrews had an increased A $\beta_{42}$  / A $\beta_{40}$  ratio in the cortical tissues as compared to the adult tree shrews (Fig. 2a, b). In line with this observation in the cortex tissues, there was an increasing trend of A $\beta_{42}$  / A $\beta_{40}$  ratio in the hippocampus tissues of the aged group (Fig. 2c, d). Moreover, both 4G8 (A $\beta_{17-24}$ ) and total A $\beta$  protein levels were also significantly increased in the cortex and hippocampus tissues of the aged tree shrews compared to adult tree shrews (Fig. 2a–d). Immunofluorescence staining showed that aged tree shrews had substantially more 4G8-positive deposits in the hippocampus and cortex tissues than in the same tissues of adult tree shrews (Fig. 2e). Furthermore, intense 4G8 immunostaining deposits in cells of the hippocampus tissue were found mainly in the CA2 region of the hippocampus (CA2) and CA3 region of the hippocampus (CA3), but not in the dentate gyrus of the hippocampus (DG) region in the aged tree shrews (Fig. 2e). This observation was confirmed by the immunohistochemical staining of CA2 and CA3 regions, where a higher number of 4G8-positive cells were observed in the aged tree shrews as compared to the adult tree shrews (Fig. 2f, g). Similar to our previous result [16], we observed only intracellular A $\beta$  accumulation, and no extracellular formed A $\beta$  plaque structures in the brain tissue of the aged tree shrews.

### Increased Phosphorylated Tau Protein in the Cortex and Hippocampus Tissues of the Aged Tree Shrews

The presence of hyperphosphorylated tau is another important feature of AD [1, 2, 4]. We examined whether the aged tree shrews had increased levels of phosphorylated tau by using

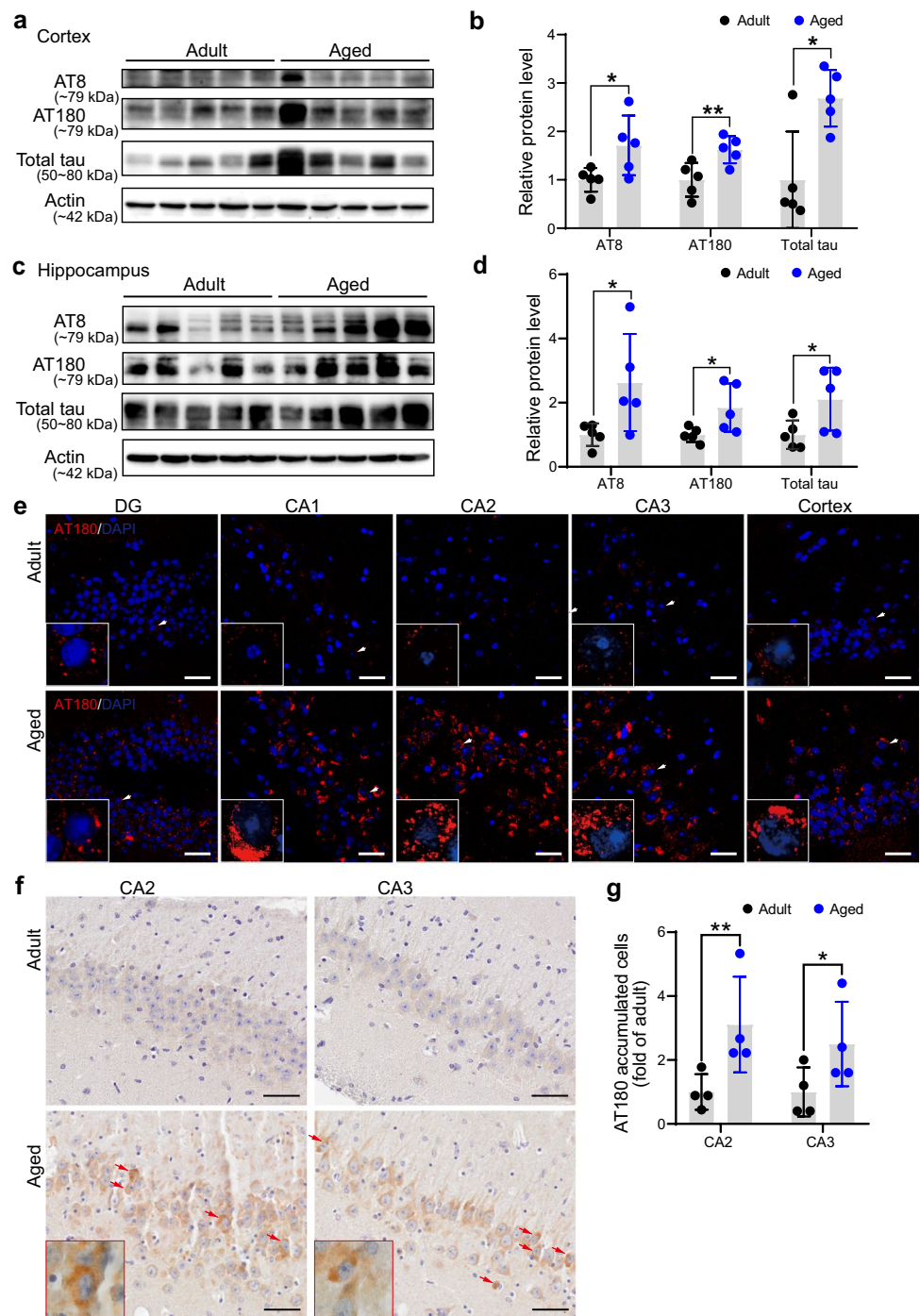
**Fig. 2** Accumulation of A $\beta$  in the cortex and hippocampus tissues of the adult and aged tree shrews. **a** Western blots for A $\beta_{40}$ , A $\beta_{42}$ , 4G8, and total-A $\beta$  in the cortex tissues of the adult and aged tree shrews. **b** Quantification of the A $\beta_{42}$ /A $\beta_{40}$  ratio (*left*), 4G8 protein level (*middle*), and total A $\beta$  protein level (*right*) in **a**. **c** Western blots for A $\beta_{40}$ , A $\beta_{42}$ , 4G8, and total-A $\beta$  in the hippocampus tissues of the adult and aged tree shrews. **d** Quantification of the A $\beta_{42}$ /A $\beta_{40}$  ratio (*left*), 4G8 protein level (*middle*), and total A $\beta$  protein level (*right*) in **c**. Actin was used as loading control; each protein level was normalized to actin. Data normalized to the adult group and represented as mean  $\pm$  SD,  $n = 5$  per group. \* $P < 0.05$ ; \*\* $P < 0.01$ ; \*\*\* $P < 0.001$  vs adult group, two-tailed unpaired Student's  $t$  test. **e** Representative images of 4G8 immunofluorescent staining for the hippocampus and cortex tissues of the adult and aged tree shrews. Scale bar, 20  $\mu$ m. The enlarged image at the left boxed area referred to the cell marked by a white arrow. **f** Representative images of 4G8 immunohistochemical staining in the CA2 and CA3 regions of the hippocampus in the adult and aged tree shrews. Scale bar, 100  $\mu$ m. **g** Quantification of 4G8 positive cells in the CA2 and CA3 regions in 5 adult and 5 aged tree shrews. Cell number in each individual was normalized to the average number of cells in the adult group and represented as mean  $\pm$  SD. \* $P < 0.05$ ; \*\* $P < 0.01$  vs adult group, two-tailed unpaired Student's  $t$  test. Red arrows indicated cells with abundant 4G8 protein accumulation, with an enlarged image of a representative cell at the left boxed area



two commonly used antibodies, AT8 and AT180. The AT8 antibody detects phosphorylation at Ser202/Thr205, while the AT180 antibody binds specifically to phosphorylated Thr231 of tau. These three phosphorylation sites are commonly involved in AD pathology [70]. Our results showed that the levels of phosphorylated tau and total tau were significantly higher in the cortex tissues of the aged tree shrews than in the

adult tree shrews (Fig. 3a, b). Consistent with the results from the cortical tissues, the protein levels of AT8, AT180 and total tau were also significantly elevated in the hippocampal tissues of the aged tree shrews as compared to those of the adult tree shrews (Fig. 3c, d). Immunofluorescence staining of the brain tissues showed that the aged tree shrews had a remarkably increased number of AT180-accumulated cells in the DG,

**Fig. 3** Tau protein level in the cortex and hippocampus tissues of the adult and aged tree shrews. **a** Western blots for AT8, AT180, and total tau in the cortex tissues of the adult and aged tree shrews. *n* = 5 per group. **b** Quantification of AT8 (left), AT180 (middle), and total tau protein level (right) in (a). **c** Western blots for AT8, AT180, and total tau in the hippocampus tissues (*n* = 5 per group). **d** Quantification of AT8 (left), AT180 (middle), and total tau protein level (right) in (c). Actin was used as the loading control; each protein level was normalized to actin. Data normalized to the adult group and represented as mean  $\pm$  SD, \**P* < 0.05; \*\**P* < 0.01 vs adult group, two-tailed unpaired Student's *t* test. **e** Representative images of AT180 immunofluorescent staining in the hippocampus and cortex tissues of the adult and aged tree shrews. Scale bar, 20  $\mu$ m. The enlarged image at the left boxed area referred to the cell marked by a white arrow. **f** Representative images of AT180 immunohistochemical staining in the CA2 and CA3 regions of the hippocampus in the adult and aged tree shrews. Scale bar, 100  $\mu$ m. **g** Quantification of AT180-positive cells in the CA2 and CA3 regions in 4 adult and 4 aged tree shrews. Cell number in each individual normalized to the average number of cells in the adult group and was represented as mean  $\pm$  SD. \**P* < 0.05; \*\**P* < 0.01 vs adult group, two-tailed unpaired Student's *t* test. Red arrows indicated cells with massive AT180 protein accumulation, with an enlarged image of a representative cell at the left boxed area

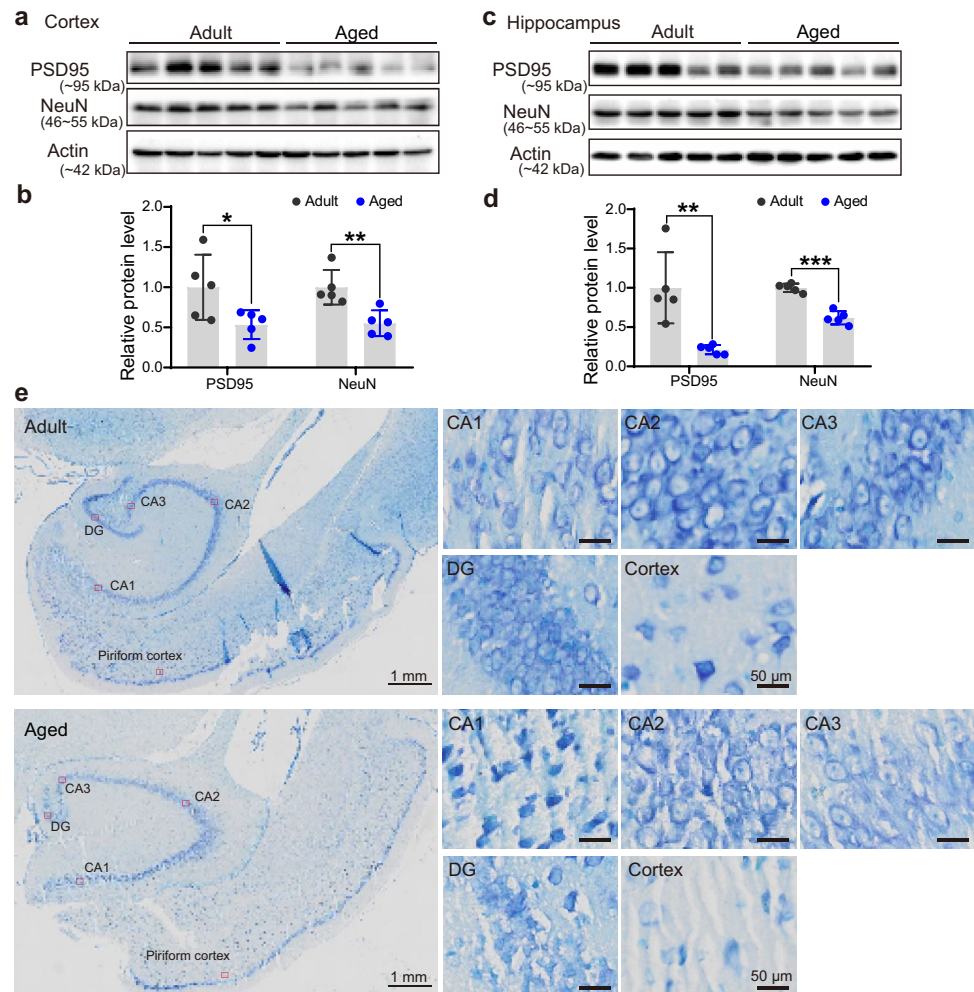


CA1 field of the hippocampus (CA1), CA2, CA3 regions of the hippocampus, and in the cortical tissues compared to the adult tree shrews (Fig. 3e). This result was validated by immunohistochemical staining, as the CA2 and CA3 regions of the hippocampus tissues of the aged tree shrews had significantly accumulated AT180 protein as compared to those of the adult tree shrews (Fig. 3f, g). Taken together, we observed increased levels of phosphorylated tau, but no typical NFTs structure, in the brain tissue of the aged tree shrews.

### The Aged Tree Shrews had Synaptic Degeneration and Neuronal Loss in the Cortex and Hippocampus Tissues

Synaptic degeneration and neuronal loss are prominent pathological features of AD at the cellular level [1, 2, 4]. We detected a severe reduction of the level of PSD-95 protein, a post-synaptic marker [71], in both cortex and hippocampal tissue of the aged tree shrews as compared to that of the adult

**Fig. 4** Synaptic degeneration and neuronal loss in the cortex and hippocampus tissues of the adult and aged tree shrews. **a** Western blots for PSD95 and NeuN in the cortex tissues of the adult and aged tree shrews.  $n = 5$  per group. **b** Quantification of PSD95 (left) and NeuN (right) protein levels in **a**. **c** Western blots for PSD95 and NeuN in the hippocampus tissues of the adult and aged tree shrews.  $n = 5$  per group. **d** Quantification of PSD95 (left) and NeuN (right) protein levels in **c**. Actin was used as loading control; each protein level was normalized to actin. Data normalized to the average of the adult group and represented as mean  $\pm$  SD,  $*P < 0.05$ ;  $**P < 0.01$ ;  $***P < 0.001$  vs adult group, two-tailed unpaired Student's  $t$  test. **e** Representative images of Nissl staining of the hippocampus in adult and aged tree shrews. Scale bar, 1 mm (whole section) or 50  $\mu$ m (enlarged section from left red rectangle)



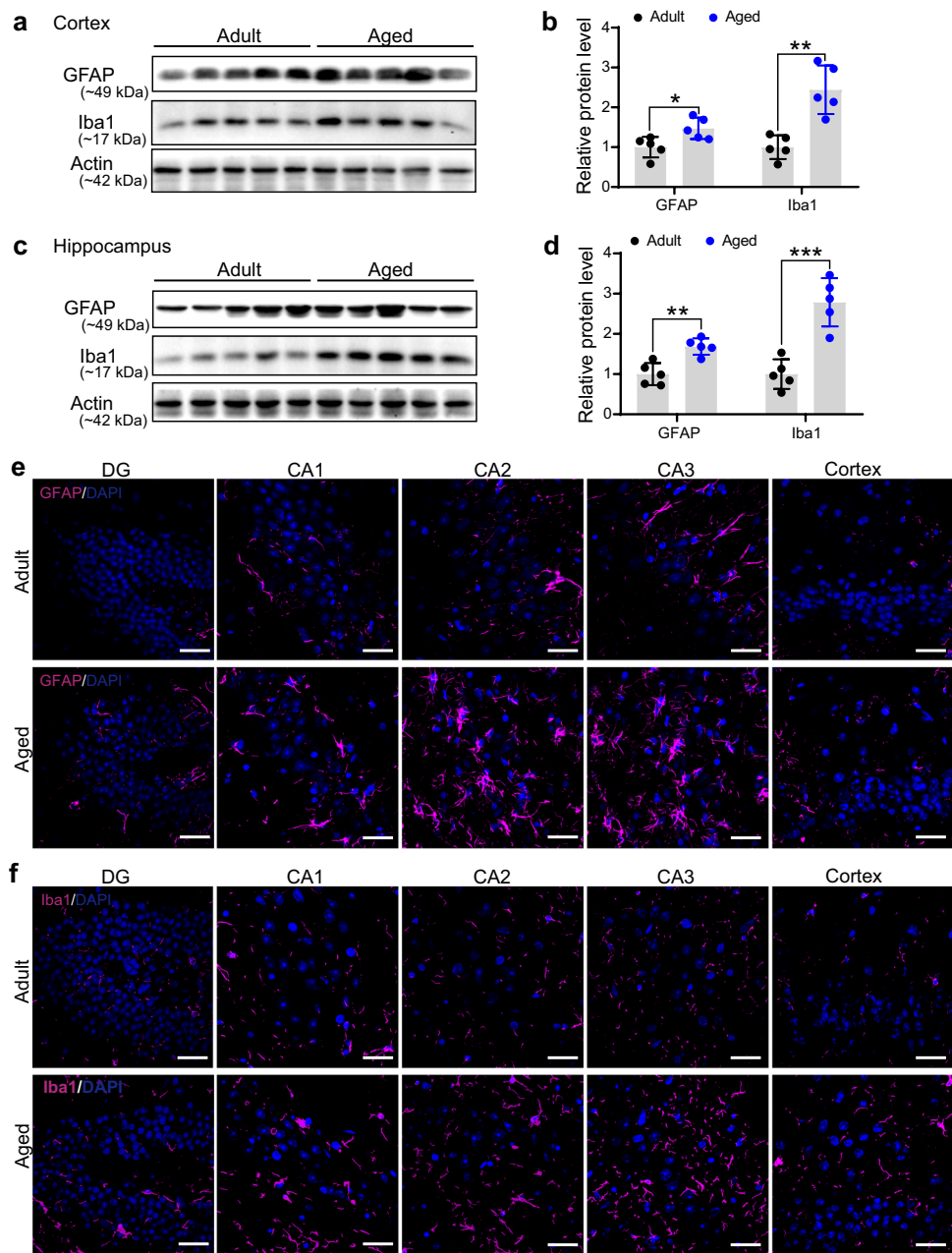
individuals (Fig. 4a–d), suggesting that synaptic degeneration occurred in the brain of tree shrews during the aging process. Similarly, the protein level of NeuN, a neuronal marker [72], was also markedly decreased in both the cortex and hippocampus of the aged tree shrews as compared to that of the adult tree shrews (Fig. 4a–d). Nissl staining of the hippocampus subregions revealed smaller and fewer holomorphic Nissl bodies in the CA1, CA2, CA3, and DG regions, and in the cortex of the aged tree shrews (Fig. 4e). This result was consistent with the results of Western blot analysis and suggested that significant neuronal loss occurs during aging.

### Enhanced Gliosis in the Cortex and Hippocampus Tissues of the Aged Tree Shrews

Neuroinflammation plays a key role in the neurodegenerative process of AD and generally constitutes the third core feature of AD neuropathology [1, 2, 4, 73–76]. Previous studies have reported a profound gliosis in the brain tissues of an AD animal model [77] and AD patients [78]. To test whether

gliosis is present in the brain of the aged tree shrews, we examined the protein levels of GFAP (an astrocyte marker) and Iba1 (a microglia marker) in the cortex and hippocampus tissues of the adult and aged animals. Western blot analyses showed a significant increase in the protein levels of GFAP and Iba1 in the cortex and hippocampus tissues of the aged animals compared to the adult individuals (Fig. 5a–d). Immunofluorescent analyses displayed an increased signal of GFAP and Iba1, as indicated by the high number of positive cells found in the hippocampus and cortex of the aged tree shrews (Fig. 5e and f). Similarly, immunohistochemical staining confirmed this pattern, with more positively stained astrocytes in the DG, CA1, CA2, and CA3 regions of the hippocampus and cortex of the aged tree shrews compared to the adult tree shrews (Fig. 6a and b). Staining for microglia showed a significant increase in the number of microglia located in the CA1 and CA2 regions of the hippocampus and the cortex tissues of the aged tree shrew as compared to the adult tree shrews (Fig. 6c and d). Consistent with a previous study showing increased total number of Iba1-positive cells

**Fig. 5** Enhanced gliosis in the cortex and hippocampus tissues of the adult and aged tree shrews. **a** Western blots for GFAP and Iba1 in the cortex tissues of the adult and aged tree shrews.  $n=5$  per group. **b** Quantification of GFAP (left) and Iba1 (right) protein levels in **a**. **c** Western blots for GFAP and Iba1 in the hippocampus tissues of the adult and aged tree shrews.  $n=5$  per group. **d** Quantification of GFAP (left) and Iba1 (right) protein level in **c**. Actin was used as loading control; each protein level was normalized to actin. Data normalized to the adult group and represented as mean  $\pm$  SD,  $*P < 0.05$ ;  $**P < 0.01$ ;  $***P < 0.001$  vs adult group, two-tailed unpaired Student's  $t$  test,  $n=5$  per group. **e, f** Representative images of GFAP (**e**) and Iba1 (**f**) immunofluorescent staining of the hippocampus and cortex tissues in the adult and aged tree shrews. Scale bar, 20  $\mu$ m



in the hippocampus of the aged tree shrews [59], our results also demonstrated an enhanced gliosis in the brain of the aged tree shrews.

## Discussion

The main pathological changes in AD are the presence of extracellular A $\beta$  plaques, intracellular NFTs, neuroinflammation, and extensive synaptic and neuronal loss in the cerebral cortex and hippocampus [1, 2, 4]. In this study, we observed impaired cognition performance, accompanied by increased levels of A $\beta$  accumulation and phosphorylated tau

protein, synaptic and neuronal loss, and gliosis in the cortex and hippocampus in the aged tree shrews as compared to the adult individuals. However, we did not observe the classic extracellular A $\beta$  plaques and typical NFTs in any of the aged tree shrews studied. This result would suggest that these typical pathological features may not be present in the aged tree shrews, or that the sample size studied is insufficient to identify these pathological features that may be rather uncommon in the tree shrews. Another possibility is that the aged tree shrews (with a mean age of less than 7 years) studied were not old enough to develop A $\beta$  plaques and typical NFTs. In addition, we may need to use more sensitive methods, such as the high-quality immunoelectron

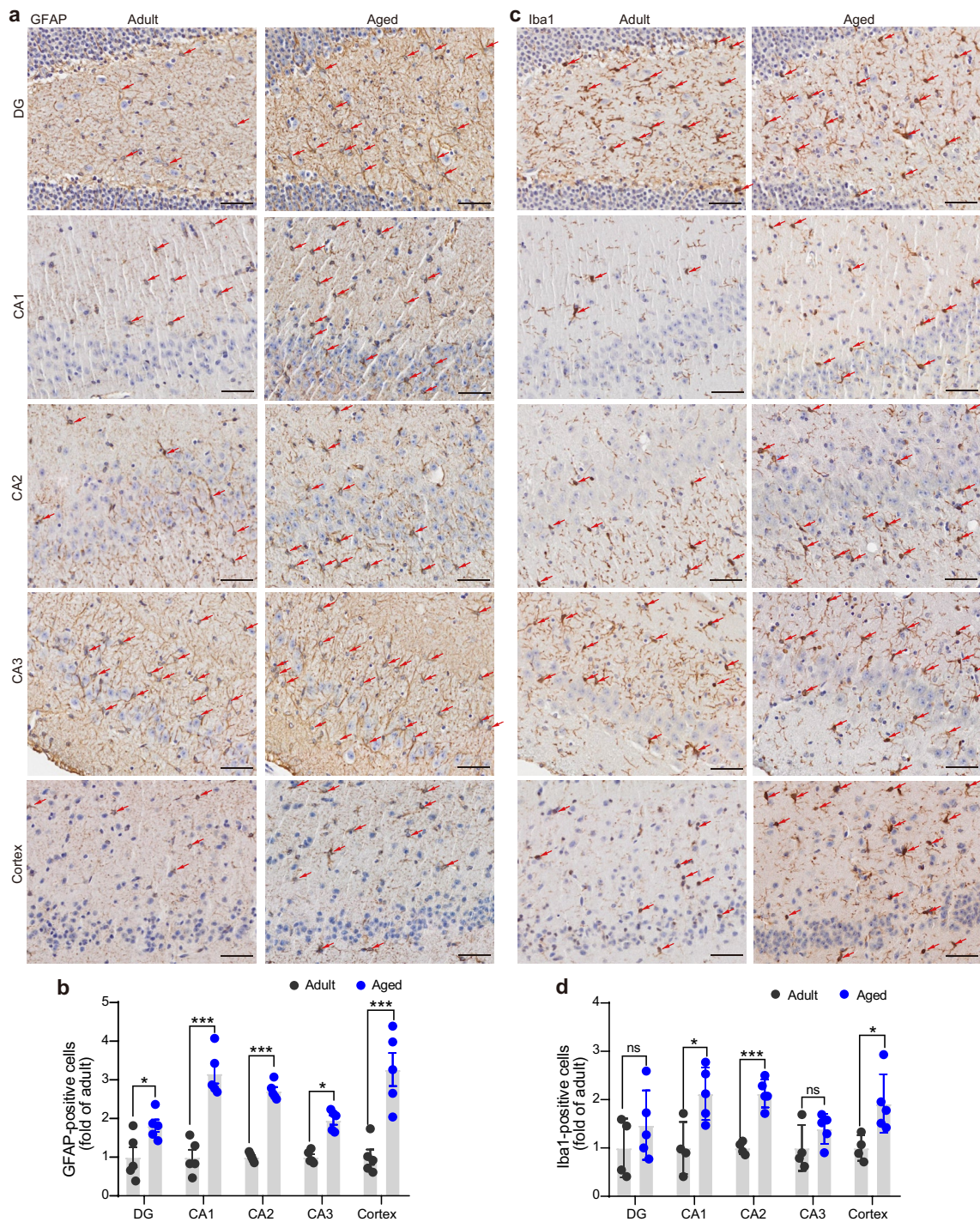


**Fig. 6** Immunohistochemical staining showing astrocytes and glia cells in the cortex and hippocampus tissues of the adult and aged tree shrews. **a, b** Representative images (**a**) and quantification (**b**) of GFAP immunohistochemical staining in the hippocampus and cortex tissues of 5 adult and 5 aged tree shrews. Scale bar, 100  $\mu$ m. Red arrows indicated GFAP positive cells. **c, d** Representative images (**c**)

and quantification (**d**) of Iba1 immunohistochemical staining in the hippocampus tissues of 4 adult and 5 aged tree shrews. Scale bar, 100  $\mu$ m. Red arrows indicated Iba1-positive cells. Cell number in each individual normalized to the average number of cells in the adult group and represented as mean  $\pm$  SD. ns, no significant; \* $P < 0.05$ ; \*\*\* $P < 0.001$  vs adult group, two-tailed unpaired Student's *t* test

microscopy studies [25, 79] and continual visualization of NFT maturity in AD [80], in order to detect these pathological features in the aged tree shrews.

AD is a neurological disorder characterized by progressive memory loss and cognitive impairment [1, 2, 5, 81]. During the aging process, human and non-human primates naturally develop age-related cognitive decline (learning and memory, forgetfulness, distractibility, inflexibility, and impaired executive functions) [79, 82–84]. In addition, aged dogs [85], rats [86, 87], mice [88, 89], and degus [90] have exhibited a decline in their memory and learning ability. Together with previous observations [66], we observed an attenuated cognitive performance in the tree shrews during aging. This result suggested that the tree shrew may be a good animal model for studying the effects of aging on cognitive performance.

Evidence suggested that the deposition of A $\beta$ <sub>42</sub> peptide, the major component of senile plaques, is significantly increased and retained in the AD brain, driving the imminent onset or progression of AD [91]. Although cerebral A $\beta$  plaques are one of the key pathologies of AD [1, 2, 4], abundant A $\beta$  deposits also occur spontaneously in the brains of many healthy people by an advanced age. Progressive cerebral deposition of A $\beta$  (including classic plaques, diffuse and primitive type) occurs in mammals (e.g., horses [92], cattle [93], polar bear [94], American black bear [95], wolverine [96], seal, sea lion, walrus [97], monkeys [98–100], camel [101], dogs [85, 102, 103], domestic cats [104]), but not in mice and rats [105, 106]. Consistent with our previous study [16], the total A $\beta$  protein levels were notably increased in the cortex and hippocampus of the aged tree shrews, but no typical plaques were observed. The A $\beta$  accumulation in aged tree shrews is similar to the diffused A $\beta$  deposits in the hippocampus tissues of the aged cats [104], suggesting a possible ability to form senile plaques.

Another key neuropathological feature of AD is hyperphosphorylated tau forming NFTs [1, 2, 4]. Similar to the A $\beta$  pathology, many mammals have been shown to naturally accumulate phosphorylated tau aggregates forming structural NFTs, including aged sheep and goats [107–109], wolverines and polar bears [94, 96], domestic cats [104], nonhuman primates (grivets and *Macaca* genus, chimpanzee, rhesus monkeys) [110, 111]. While tau accumulation occurred in aging horses [92], pinniped species (seal, sea lion, and walrus) naturally accumulated hyperphosphorylated tau during aging [97]. Furthermore, aged cats and dogs also showed neuronal loss [102, 104]. In addition to non-human primates [112], senile dogs also showed significant cortical atrophy, accompanied by an increase in ventricular volume [85, 102, 103]. Similar to these naturally aging animals, we observed profound phosphorylated tau in aged tree shrews. We have also observed a severe cortical atrophy

and expanded ventricular volume under the microscope in a 6.2-year-old tree shrew (data not shown).

Activation of glial cells, including microglia and astrocytes, plays an important role in triggering the inflammatory signaling pathways involved in AD [2, 4, 76], leading to the inflammation hypothesis of sporadic late-onset AD [113]. Based on this hypothesis, the natural neuronal response to inflammatory stress includes hyperphosphorylated tau, mislocated hyperphosphorylated tau, and increased APP expression [113]. Moderate activation of neuroprotective microglia facilitates the clearance of the A $\beta$  aggregates under physiological conditions. However, in the setting of pathological aging, such as overweight and obesity in mid-life, microglia become hyper-reactive to induce an exaggerated neuroprotective inflammatory response, resulting in neuronal damage (e.g., disruption of the axonal cytoskeleton contributing to the impaired axonal transport, formation of axonal swellings of APP aggregates, and dystrophic neurites) that cannot be cleared by hyper-reactive microglia [114, 115]. Secondary to the neuronal degeneration, A $\beta$  plaques are formed from the intracellular APP aggregates, triggering further release of proinflammatory molecules that exacerbate the neurodegenerative processes in AD [114–116]. Recently, it has been suggested that chronic neuroinflammation may be a precursor to the development of A $\beta$  and tau pathology in sporadic AD [117]. Therefore, an animal model based on the inflammatory hypothesis of sporadic AD should include the following features: (a) primary chronic neuroinflammation [117], (b) memory and cognitive impairment, and (c) tau and A $\beta$  pathology [114]. Obviously, the tree shrew may be a suitable animal model to study the inflammatory hypothesis of sporadic AD based on the observed activation of glial cells during aging.

The current study has several limitations. First, we did not detect all related biomarkers of aging in the aged tree shrews [118] and perform an association between these biomarkers of aging with the observed cognitive impairments during aging. Second, the evaluation for aging-associated behavioral changes may be insufficient for defining the cognitive impairment in the aged tree shrews. More behavioral paradigms and physiological tests for the tree shrews should be designed and optimized to validate the same as a standard test animal for AD and aging in the future.

## Conclusion and Outlook

In the present study, we performed a comparison of AD pathological features in the adult and aged tree shrews. We found impaired cognitive performance, accompanied by increased levels of intracellular A $\beta$  accumulation and phosphorylated tau protein, synaptic and neuronal loss, and gliosis in the

cortex and hippocampus of the aged tree shrews. These findings indicated that the tree shrews accumulate AD-related pathologies during aging and have the potential to be an optimal experimental animal model for AD research. In the future, more studies should be carried out to investigate whether the accumulated A $\beta$  and phosphorylated tau in brain of the tree shrews could further develop to typical A $\beta$  plaques and NFTs naturally or through acquired factors (e.g., metabolic disorders and virus infections). Collectively, this study has provided the molecular basis to show that the tree shrew is a potential model for research in AD and aging-related diseases.

**Abbreviations** AD: Alzheimer's disease; A $\beta$ : Amyloid- $\beta$ ; NFTs: Neurofibrillary tangles; MAPT: Microtubule-associated protein tau; PBS: Phosphate-buffered saline; BSA: Bovine serum albumin; SDS-PAGE: Sodium dodecyl sulfate–polyacrylamide gel electrophoresis; DG: Dentate gyrus of the hippocampus; CA1: Field CA2 of hippocampus; CA2: CA2 region of hippocampus; CA3: CA3 region of the hippocampus

**Acknowledgements** We thank Dr. Ian Logan for help with the language editing and helpful comments.

**Author Contribution** YGY, RB, PZ, and HLL designed the study; HLL, BLX, XL, CL, YL, YM, and GLM performed the experiments and data analysis; JQC, QYZ, and LBL conducted and provided the animals; HLL wrote the manuscript and prepared the figures, YGY and RB provided advice and edited the manuscript. All authors read and approved the final manuscript.

**Funding** This study was supported by the Ministry of Science and Technology of China (2021YFF0702700 and 2021ZD0200901), the National Natural Science Foundation of China (82301634, U1902215 and U1702284), the Chinese Academy of Sciences (Light of West China Program xbgz-zdsys-201909), Yunnan province (202301AT070322), and the Youth Innovation Promotion Association of CAS (2020000017).

**Data Availability** The data supporting the findings of this study are available within the article.

## Declarations

**Ethics Approval and Consent to Participate** In this study, all animal experiments were approved in compliance with the Animal Ethics Committee of the Kunming Institute of Zoology, Chinese Academy of Science (Approval number: IACUC18027).

**Consent for Publication** Not applicable.

**Competing Interests** The authors declare no competing interests.

## References

- Querfurth HW, LaFerla FM (2010) Alzheimer's disease. *N Engl J Med* 362:329–344. <https://doi.org/10.1056/NEJMra0909142>
- Scheltens P, De Strooper B, Kivipelto M, Holstege H, Chételat G, Teunissen CE et al (2021) Alzheimer's disease. *Lancet* 397:1577–1590. [https://doi.org/10.1016/s0140-6736\(20\)32205-4](https://doi.org/10.1016/s0140-6736(20)32205-4)
- Alzheimer's Association (2023) 2023 Alzheimer's disease facts and figures. *Alzheimers Dement* 19:1598–1695. <https://doi.org/10.1002/alz.13016>
- De Strooper B, Karran E (2016) The cellular phase of Alzheimer's disease. *Cell* 164:603–615. <https://doi.org/10.1016/j.cell.2015.12.056>
- Knopman DS, Amieva H, Petersen RC, Chételat G, Holtzman DM, Hyman BT et al (2021) Alzheimer disease. *Nat Rev Dis Primers* 7:33. <https://doi.org/10.1038/s41572-021-00269-y>
- Zhang Y, Chen H, Li R, Sterling K, Song W (2023) Amyloid  $\beta$ -based therapy for Alzheimer's disease: challenges, successes and future. *Signal Transduct Target Ther* 8:248. <https://doi.org/10.1038/s41392-023-01484-7>
- Hodson R (2018) Alzheimer's disease. *Nature* 559:S1. <https://doi.org/10.1038/d41586-018-05717-6>
- Khoramipour K, Bejeshk MA, Rajizadeh MA, Najafipour H, Dehghan P, Farahmand F (2023) High-intensity interval training ameliorates molecular changes in the hippocampus of male rats with the diabetic brain: the role of adiponectin. *Mol Neurobiol* 60:3486–3495. <https://doi.org/10.1007/s12035-023-03285-z>
- Sharma R, Kuca K, Nepovimova E, Kabra A, Rao MM, Prajapati PK (2019) Traditional Ayurvedic and herbal remedies for Alzheimer's disease: from bench to bedside. *Expert Rev Neurother* 19:359–374. <https://doi.org/10.1080/14737175.2019.1596803>
- Xie C, Zhuang XX, Niu Z, Ai R, Lautrup S, Zheng S et al (2022) Amelioration of Alzheimer's disease pathology by mitophagy inducers identified via machine learning and a cross-species workflow. *Nat Biomed Eng* 6:76–93. <https://doi.org/10.1038/s41551-021-00819-5>
- Yang L, Deng YT, Leng Y, Ou YN, Li YZ, Chen SD et al (2023) Depression, depression treatments, and risk of incident dementia: a prospective cohort study of 354,313 participants. *Biol Psychiatry* 93:802–809. <https://doi.org/10.1016/j.biopsych.2022.08.026>
- Wang ZB, Wang ZT, Sun Y, Tan L, Yu JT (2022) The future of stem cell therapies of Alzheimer's disease. *Ageing Res Rev* 80:101655. <https://doi.org/10.1016/j.arr.2022.101655>
- Luo R, Su LY, Li G, Yang J, Liu Q, Yang LX et al (2020) Activation of PPARA-mediated autophagy reduces Alzheimer disease-like pathology and cognitive decline in a murine model. *Autophagy* 16:52–69. <https://doi.org/10.1080/15548627.2019.1596488>
- Chen ZY, Zhang Y (2022) Animal models of Alzheimer's disease: applications, evaluation, and perspectives. *Zool Res* 43:1026–1040. <https://doi.org/10.24272/j.issn.2095-8137.2022.289>
- Drummond E, Wisniewski T (2017) Alzheimer's disease: experimental models and reality. *Acta Neuropathol* 133:155–175. <https://doi.org/10.1007/s00401-016-1662-x>
- Fan Y, Luo R, Su LY, Xiang Q, Yu D, Xu L et al (2018) Does the genetic feature of the Chinese tree shrew (*Tupaia belangeri chinensis*) support its potential as a viable model for Alzheimer's disease research? *J Alzheimers Dis* 61:1015–1028. <https://doi.org/10.3233/jad-170594>
- Reardon S (2018) Frustrated Alzheimer's researchers seek better lab mice. *Nature* 563:611–612. <https://doi.org/10.1038/d41586-018-07484-w>
- Beckman D, Chakrabarty P, Ott S, Dao A, Zhou E, Janssen WG et al (2021) A novel tau-based rhesus monkey model of Alzheimer's pathogenesis. *Alzheimers Dement* 17:933–945. <https://doi.org/10.1002/alz.12318>
- Wang ZH, Xia Y, Wu Z, Kang SS, Zhang JC, Liu P et al (2022) Neuronal ApoE4 stimulates C/EBP $\beta$  activation, promoting Alzheimer's disease pathology in a mouse model. *Prog Neurobiol* 209:102212. <https://doi.org/10.1016/j.pneurobio.2021.102212>
- Pang K, Jiang R, Zhang W, Yang Z, Li LL, Shimozaawa M et al (2022) An App knock-in rat model for Alzheimer's disease exhibiting A $\beta$  and tau pathologies, neuronal death and cognitive

- impairments. *Cell Res* 32:157–175. <https://doi.org/10.1038/s41422-021-00582-x>
21. Barendrecht S, Schreurs A, Geissler S, Sabanov V, Ilse V, Rieckmann V et al (2023) A novel human tau knock-in mouse model reveals interaction of Abeta and human tau under progressing cerebral amyloidosis in 5xFAD mice. *Alzheimers Res Ther* 15:16. <https://doi.org/10.1186/s13195-022-01144-y>
  22. Kim TA, Syty MD, Wu K, Ge S (2022) Adult hippocampal neurogenesis and its impairment in Alzheimer's disease. *Zool Res* 43:481–496. <https://doi.org/10.24272/j.issn.2095-8137.2021.479>
  23. Li ZH, He XP, Li H, He RQ, Hu XT (2020) Age-associated changes in amyloid- $\beta$  and formaldehyde concentrations in cerebrospinal fluid of rhesus monkeys. *Zool Res* 41:444–448. <https://doi.org/10.24272/j.issn.2095-8137.2020.088>
  24. Frye BM, Craft S, Register TC, Andrews RN, Appt SE, Vitolins MZ et al (2021) Diet, psychosocial stress, and Alzheimer's disease-related neuroanatomy in female nonhuman primates. *Alzheimers Dement* 17:733–744. <https://doi.org/10.1002/alz.12232>
  25. Paspalas CD, Carlyle BC, Leslie S, Preuss TM, Crimins JL, Huttner AJ et al (2018) The aged rhesus macaque manifests Braak stage III/IV Alzheimer's-like pathology. *Alzheimers Dement* 14:680–691. <https://doi.org/10.1016/j.jalz.2017.11.005>
  26. Gunn-Moore D, Kaidanovich-Beilin O, Gallego Iradi MC, Gunn-Moore F, Lovestone S (2018) Alzheimer's disease in humans and other animals: a consequence of postreproductive life span and longevity rather than aging. *Alzheimers Dement* 14:195–204. <https://doi.org/10.1016/j.jalz.2017.08.014>
  27. Li HW, Zhang L, Qin C (2019) Current state of research on non-human primate models of Alzheimer's disease. *Animal Model Exp Med* 2:227–238. <https://doi.org/10.1002/ame2.12092>
  28. Roelfsema PR, Treue S (2014) Basic neuroscience research with nonhuman primates: a small but indispensable component of biomedical research. *Neuron* 82:1200–1204. <https://doi.org/10.1016/j.neuron.2014.06.003>
  29. Xiao J, Liu R, Chen CS (2017) Tree shrew (*Tupaia belangeri*) as a novel laboratory disease animal model. *Zool Res* 38:127–137. <https://doi.org/10.24272/j.issn.2095-8137.2017.033>
  30. Yao YG (2017) Creating animal models, why not use the Chinese tree shrew (*Tupaia belangeri chinensis*)? *Zool Res* 38:118–126. <https://doi.org/10.24272/j.issn.2095-8137.2017.032>
  31. Xu L, Chen SY, Nie WH, Jiang XL, Yao YG (2012) Evaluating the phylogenetic position of Chinese tree shrew (*Tupaia belangeri chinensis*) based on complete mitochondrial genome: implication for using tree shrew as an alternative experimental animal to primates in biomedical research. *J Genet Genomics* 39:131–137. <https://doi.org/10.1016/j.jgg.2012.02.003>
  32. Fan Y, Huang ZY, Cao CC, Chen CS, Chen YX, Fan DD et al (2013) Genome of the Chinese tree shrew. *Nat Commun* 4:1426. <https://doi.org/10.1038/ncomms2416>
  33. Fan Y, Ye MS, Zhang JY, Xu L, Yu DD, Gu TL et al (2019) Chromosomal level assembly and population sequencing of the Chinese tree shrew genome. *Zool Res* 40:506–521. <https://doi.org/10.24272/j.issn.2095-8137.2019.063>
  34. Ye MS, Zhang JY, Yu DD, Xu M, Xu L, Lv LB et al (2021) Comprehensive annotation of the Chinese tree shrew genome by large-scale RNA sequencing and long-read isoform sequencing. *Zool Res* 42:692–709. <https://doi.org/10.24272/j.issn.2095-8137.2021.272>
  35. Xu L, Yu DD, Ma YH, Yao YL, Luo RH, Feng XL et al (2020) COVID-19-like symptoms observed in Chinese tree shrews infected with SARS-CoV-2. *Zool Res* 41:517–526. <https://doi.org/10.24272/j.issn.2095-8137.2020.053>
  36. Ohl F, Oitzl MS, Fuchs E (1998) Assessing cognitive functions in tree shrews: visuo-spatial and spatial learning in the home cage. *J Neurosci Methods* 81:35–40. [https://doi.org/10.1016/s0165-0270\(98\)00011-9](https://doi.org/10.1016/s0165-0270(98)00011-9)
  37. Pan TT, Liu C, Li DM, Nie BB, Zhang TH, Zhang W et al (2022) Nucleus accumbens-linked executive control networks mediating reversal learning in tree shrew brain. *Zool Res* 43:528–531. <https://doi.org/10.24272/j.issn.2095-8137.2022.063>
  38. Savier E, Sedigh-Sarvestani M, Wimmer R, Fitzpatrick D (2021) A bright future for the tree shrew in neuroscience research: summary from the inaugural tree shrew users meeting. *Zool Res* 42:478–481. <https://doi.org/10.24272/j.issn.2095-8137.2021.178>
  39. Chen Q, Ma ZX, Xia LB, Ye ZN, Liu BL, Ma TK et al (2020) A tree shrew model for steroid-associated osteonecrosis. *Zool Res* 41:564–568. <https://doi.org/10.24272/j.issn.2095-8137.2020.061>
  40. Sun J, Liu W, Guo Y, Zhang H, Jiang D, Luo Y et al (2021) Characterization of tree shrew telomeres and telomerase. *J Genet Genomics* 48:631–639. <https://doi.org/10.1016/j.jgg.2021.06.004>
  41. Xia W, Chen H, Feng Y, Shi N, Huang Z, Feng Q et al (2021) Tree shrew is a suitable animal model for the study of Epstein Barr virus. *Front Immunol* 12:789604. <https://doi.org/10.3389/fimmu.2021.789604>
  42. Gorbatyuk OS, Pitale PM, Saltykova IV, Dorofeeva IB, Zhylkibayev AA, Athar M et al (2021) A novel tree shrew model of diabetic retinopathy. *Front Endocrinol (Lausanne)* 12:799711. <https://doi.org/10.3389/fendo.2021.799711>
  43. Kayesh MEH, Sanada T, Kohara M, Tsukiyama-Kohara K (2021) Tree shrew as an emerging small animal model for human viral infection: a recent overview. *Viruses* 13. <https://doi.org/10.3390/v13081641>
  44. Lu T, Peng H, Zhong L, Wu P, He J, Deng Z et al (2021) The tree shrew as a model for cancer research. *Front Oncol* 11:653236. <https://doi.org/10.3389/fonc.2021.653236>
  45. Ohl F, Fuchs E (1998) Memory performance in tree shrews: effects of stressful experiences. *Neurosci Biobehav Rev* 23:319–323. [https://doi.org/10.1016/s0149-7634\(98\)00033-5](https://doi.org/10.1016/s0149-7634(98)00033-5)
  46. Yin C, Zhou X, Yao YG, Wang W, Wu Q, Wang X (2020) Abundant self-amplifying intermediate progenitors in the subventricular zone of the Chinese tree shrew neocortex. *Cereb Cortex* 30:3370–3380. <https://doi.org/10.1093/cercor/bhz315>
  47. Tanabe S, Fu J, Cang J (2022) Strong tuning for stereoscopic depth indicates orientation-specific recurrent circuitry in tree shrew V1. *Curr Biol* 32:5274–5284.e6. <https://doi.org/10.1016/j.cub.2022.10.063>
  48. Schumacher JW, McCann MK, Maximov KJ, Fitzpatrick D (2022) Selective enhancement of neural coding in V1 underlies fine-discrimination learning in tree shrew. *Curr Biol* 32:3245–3260.e5. <https://doi.org/10.1016/j.cub.2022.06.009>
  49. Petry HM, Bickford ME (2019) The second visual system of the tree shrew. *J Comp Neurol* 527:679–693. <https://doi.org/10.1002/cne.24413>
  50. De Luna P, Veit J, Rainer G (2017) Basal forebrain activation enhances between-trial reliability of low-frequency local field potentials (LFP) and spiking activity in tree shrew primary visual cortex (V1). *Brain Struct Funct* 222:4239–4252. <https://doi.org/10.1007/s00429-017-1468-1>
  51. Wei S, Hua HR, Chen QQ, Zhang Y, Chen F, Li SQ et al (2017) Dynamic changes in DNA demethylation in the tree shrew (*Tupaia belangeri chinensis*) brain during postnatal development and aging. *Zool Res* 38:96–102. <https://doi.org/10.24272/j.issn.2095-8137.2017.013>
  52. Ni RJ, Huang ZH, Luo PH, Ma XH, Li T, Zhou JN (2018) The tree shrew cerebellum atlas: Systematic nomenclature, neurochemical characterization, and afferent projections. *J Comp Neurol* 526:2744–2775. <https://doi.org/10.1002/cne.24526>
  53. Luo PH, Shu YM, Ni RJ, Liu YJ, Zhou JN (2020) A characteristic expression pattern of core circadian genes in the diurnal tree shrew. *Neuroscience* 437:145–160. <https://doi.org/10.1016/j.neuroscience.2020.04.027>
  54. Zhang J, Luo RC, Man XY, Lv LB, Yao YG, Zheng M (2020) The anatomy of the skin of the Chinese tree shrew is very similar

- to that of human skin. *Zool Res* 41:208–212. <https://doi.org/10.24272/j.issn.2095-8137.2020.028>
55. Ni RJ, Tian Y, Dai XY, Zhao LS, Wei JX, Zhou JN et al (2020) Social avoidance behavior in male tree shrews and prosocial behavior in male mice toward unfamiliar conspecifics in the laboratory. *Zool Res* 41:258–272. <https://doi.org/10.24272/j.issn.2095-8137.2020.034>
  56. Pawlik M, Fuchs E, Walker LC, Levy E (1999) Primate-like amyloid-beta sequence but no cerebral amyloidosis in aged tree shrews. *Neurobiol Aging* 20:47–51. [https://doi.org/10.1016/s0197-4580\(99\)00017-2](https://doi.org/10.1016/s0197-4580(99)00017-2)
  57. Yamashita A, Fuchs E, Taira M, Hayashi M (2010) Amyloid beta (A $\beta$ ) protein- and amyloid precursor protein (APP)-immunoreactive structures in the brains of aged tree shrews. *Curr Aging Sci* 3:230–238. <https://doi.org/10.2174/1874609811003030230>
  58. Yamashita A, Fuchs E, Taira M, Yamamoto T, Hayashi M (2012) Somatostatin-immunoreactive senile plaque-like structures in the frontal cortex and nucleus accumbens of aged tree shrews and Japanese macaques. *J Med Primatol* 41:147–157. <https://doi.org/10.1111/j.1600-0684.2012.00540.x>
  59. Rodríguez-Callejas JD, Fuchs E, Pérez-Cruz C (2020) Increased oxidative stress, hyperphosphorylation of tau, and dystrophic microglia in the hippocampus of aged *Tupaia belangeri*. *Glia* 68:1775–1793. <https://doi.org/10.1002/glia.23804>
  60. Lin N, Xiong LL, Zhang RP, Zheng H, Wang L, Qian ZY et al (2016) Injection of A $\beta$ 1-40 into hippocampus induced cognitive lesion associated with neuronal apoptosis and multiple gene expressions in the tree shrew. *Apoptosis* 21:621–640. <https://doi.org/10.1007/s10495-016-1227-4>
  61. Chen JQ, Zhang Q, Yu D, Bi R, Ma Y, Li Y et al (2022) Optimization of milk substitutes for the artificial rearing of Chinese tree shrews (*Tupaia belangeri chinensis*). *Animals (Basel)* 12:1655. <https://doi.org/10.3390/ani12131655>
  62. Labots M, Van Lith HA, Ohl F, Arndt SS (2015) The modified hole board—measuring behavior, cognition and social interaction in mice and rats. *J Vis Exp* 52529. <https://doi.org/10.3791/52529>
  63. Lecorps B, Woodroffe RE, von Keyserlingk MAG, Weary DM (2022) Assessing cognitive performance in dairy calves using a modified hole-board test. *Anim Cogn* 25:1365–1370. <https://doi.org/10.1007/s10071-022-01617-5>
  64. Jiao L, Su LY, Liu Q, Luo R, Qiao X, Xie T et al (2022) GSNOR deficiency attenuates MPTP-induced neurotoxicity and autophagy by facilitating CDK5 S-nitrosation in a mouse model of Parkinson's disease. *Free Radic Biol Med* 189:111–121. <https://doi.org/10.1016/j.freeradbiomed.2022.07.016>
  65. Sampedro-Piquero P, Mañas-Padilla MC, Ávila-Gámiz F, Gil-Rodríguez S, Santín LJ, Castilla-Ortega E (2019) Where to place the rewards? Exploration bias in mice influences performance in the classic hole-board spatial memory test. *Anim Cogn* 22:433–443. <https://doi.org/10.1007/s10071-019-01256-3>
  66. Keuker JJ, de Biurrun G, Luiten PG, Fuchs E (2004) Preservation of hippocampal neuron numbers and hippocampal subfield volumes in behaviorally characterized aged tree shrews. *J Comp Neurol* 468:509–517. <https://doi.org/10.1002/cne.10996>
  67. Bevins RA, Besheer J (2006) Object recognition in rats and mice: a one-trial non-matching-to-sample learning task to study “recognition memory.” *Nat Protoc* 1:1306–1311. <https://doi.org/10.1038/nprot.2006.205>
  68. Khani A, Rainer G (2012) Recognition memory in tree shrew (*Tupaia belangeri*) after repeated familiarization sessions. *Behav Processes* 90:364–371. <https://doi.org/10.1016/j.beproc.2012.03.019>
  69. Nair J, Topka M, Khani A, Isenschmid M, Rainer G (2014) Tree shrews (*Tupaia belangeri*) exhibit novelty preference in the novel location memory task with 24-h retention periods. *Front Psychol* 5:303. <https://doi.org/10.3389/fpsyg.2014.00303>
  70. Neddens J, Temmel M, Flunkert S, Kerschbaumer B, Hoeller C, Loeffler T et al (2018) Phosphorylation of different tau sites during progression of Alzheimer's disease. *Acta Neuropathol Commun* 6:52. <https://doi.org/10.1186/s40478-018-0557-6>
  71. Schnell E, Sizemore M, Karimzadegan S, Chen L, Bredt DS, Nicoll RA (2002) Direct interactions between PSD-95 and stargazin control synaptic AMPA receptor number. *Proc Natl Acad Sci U S A* 99:13902–13907. <https://doi.org/10.1073/pnas.172511199>
  72. Mullen RJ, Buck CR, Smith AM (1992) NeuN, a neuronal specific nuclear protein in vertebrates. *Development* 116:201–211. <https://doi.org/10.1242/dev.116.1.201>
  73. Ferrari C, Sorbi S (2021) The complexity of Alzheimer's disease: an evolving puzzle. *Physiol Rev* 101:1047–1081. <https://doi.org/10.1152/physrev.00015.2020>
  74. Boyd RJ, Avramopoulos D, Jantzie LL, McCallion AS (2022) Neuroinflammation represents a common theme amongst genetic and environmental risk factors for Alzheimer and Parkinson diseases. *J Neuroinflammation* 19:223. <https://doi.org/10.1186/s12974-022-02584-x>
  75. Thakur S, Dhapola R, Sarma P, Medhi B, Reddy DH (2023) Neuroinflammation in Alzheimer's disease: current progress in molecular signaling and therapeutics. *Inflammation* 46:1–17. <https://doi.org/10.1007/s10753-022-01721-1>
  76. Jorfi M, Maaser-Hecker A, Tanzi RE (2023) The neuroimmune axis of Alzheimer's disease. *Genome Med* 15:6. <https://doi.org/10.1186/s13073-023-01155-w>
  77. Yoshiyama Y, Higuchi M, Zhang B, Huang SM, Iwata N, Saido TC et al (2007) Synapse loss and microglial activation precede tangles in a P301S tauopathy mouse model. *Neuron* 53:337–351. <https://doi.org/10.1016/j.neuron.2007.01.010>
  78. Beach TG, Walker R, McGeer EG (1989) Patterns of gliosis in Alzheimer's disease and aging cerebrum. *Glia* 2:420–436. <https://doi.org/10.1002/glia.440020605>
  79. Arnsten AFT, Datta D, Leslie S, Yang ST, Wang M, Nairn AC (2019) Alzheimer's-like pathology in aging rhesus macaques: unique opportunity to study the etiology and treatment of Alzheimer's disease. *Proc Natl Acad Sci U S A* 116:26230–26238. <https://doi.org/10.1073/pnas.1903671116>
  80. Moloney CM, Lowe VJ, Murray ME (2021) Visualization of neurofibrillary tangle maturity in Alzheimer's disease: a clinicopathologic perspective for biomarker research. *Alzheimers Dement* 17:1554–1574. <https://doi.org/10.1002/alz.12321>
  81. Lyketsos CG, Carrillo MC, Ryan JM, Khachaturian AS, Trzepacz P, Amatniek J et al (2011) Neuropsychiatric symptoms in Alzheimer's disease. *Alzheimers Dement* 7:532–539. <https://doi.org/10.1016/j.jalz.2011.05.2410>
  82. Rapp PR, Amaral DG (1989) Evidence for task-dependent memory dysfunction in the aged monkey. *J Neurosci* 9:3568–3576. <https://doi.org/10.1523/jneurosci.09-10-03568.1989>
  83. Wang M, Gamo NJ, Yang Y, Jin LE, Wang XJ, Laubach M et al (2011) Neuronal basis of age-related working memory decline. *Nature* 476:210–213. <https://doi.org/10.1038/nature10243>
  84. Rypma B, D'Esposito M (2000) Isolating the neural mechanisms of age-related changes in human working memory. *Nat Neurosci* 3:509–515. <https://doi.org/10.1038/74889>
  85. Bosch MN, Pugliese M, Gimeno-Bayón J, Rodríguez MJ, Mahy N (2012) Dogs with cognitive dysfunction syndrome: a natural model of Alzheimer's disease. *Curr Alzheimer Res* 9:298–314. <https://doi.org/10.2174/156720512800107546>
  86. Gallagher M, Pelleymounter MA (1988) Spatial learning deficits in old rats: a model for memory decline in the aged. *Neurobiol Aging* 9:549–556. [https://doi.org/10.1016/s0197-4580\(88\)80112-x](https://doi.org/10.1016/s0197-4580(88)80112-x)
  87. Gage FH, Chen KS, Buzsáki G, Armstrong D (1988) Experimental approaches to age-related cognitive impairments. *Neurobiol Aging* 9:645–655. [https://doi.org/10.1016/s0197-4580\(88\)80129-5](https://doi.org/10.1016/s0197-4580(88)80129-5)
  88. Gower AJ, Lamberty Y (1993) The aged mouse as a model of cognitive decline with special emphasis on studies in NMRI

- mic. *Behav Brain Res* 57:163–173. [https://doi.org/10.1016/0166-4328\(93\)90132-a](https://doi.org/10.1016/0166-4328(93)90132-a)
89. Forster MJ, Dubey A, Dawson KM, Stutts WA, Lal H, Sohail RS (1996) Age-related losses of cognitive function and motor skills in mice are associated with oxidative protein damage in the brain. *Proc Natl Acad Sci U S A* 93:4765–4769. <https://doi.org/10.1073/pnas.93.10.4765>
  90. Rivera DS, Lindsay CB, Oliva CA, Bozinovic F, Inestrosa NC (2021) A multivariate assessment of age-related cognitive impairment in *Octodon degus*. *Front Integr Neurosci* 15:719076. <https://doi.org/10.3389/fnint.2021.719076>
  91. Hardy J, Selkoe DJ (2002) The amyloid hypothesis of Alzheimer's disease: progress and problems on the road to therapeutics. *Science* 297:353–356. <https://doi.org/10.1126/science.1072994>
  92. Capucchio MT, Márquez M, Pregel P, Foradada L, Bravo M, Matutino G et al (2010) Parenchymal and vascular lesions in ageing equine brains: histological and immunohistochemical studies. *J Comp Pathol* 142:61–73. <https://doi.org/10.1016/j.jcpa.2009.07.007>
  93. Moreno-Gonzalez I, Gr E, Morales R, Duran-Aniotz C, Escobedo G Jr, Marquez M et al (2021) Aged cattle brain displays Alzheimer's disease-like pathology and promotes brain amyloidosis in a transgenic animal model. *Front Aging Neurosci* 13:815361. <https://doi.org/10.3389/fnagi.2021.815361>
  94. Tekirian TL, Cole GM, Russell MJ, Yang F, Wekstein DR, Patel E et al (1996) Carboxy terminal of beta-amyloid deposits in aged human, canine, and polar bear brains. *Neurobiol Aging* 17:249–257. [https://doi.org/10.1016/0197-4580\(95\)02062-4](https://doi.org/10.1016/0197-4580(95)02062-4)
  95. Uchida K, Yoshino T, Yamaguchi R, Tateyama S, Kimoto Y, Nakayama H et al (1995) Senile plaques and other senile changes in the brain of an aged American black bear. *Vet Pathol* 32:412–414. <https://doi.org/10.1177/030098589503200410>
  96. Roertgen KE, Parisi JE, Clark HB, Barnes DL, O'Brien TD, Johnson KH (1996) A beta-associated cerebral angiopathy and senile plaques with neurofibrillary tangles and cerebral hemorrhage in an aged wolverine (*Gulo gulo*). *Neurobiol Aging* 17:243–247. [https://doi.org/10.1016/0197-4580\(95\)02069-1](https://doi.org/10.1016/0197-4580(95)02069-1)
  97. Takaichi Y, Chambers JK, Takahashi K, Soeda Y, Koike R, Katsumata E et al (2021) Amyloid  $\beta$  and tau pathology in brains of aged pinniped species (sea lion, seal, and walrus). *Acta Neuropathol Commun* 9:10. <https://doi.org/10.1186/s40478-020-01104-3>
  98. Latimer CS, Shively CA, Keene CD, Jorgensen MJ, Andrews RN, Register TC et al (2019) A nonhuman primate model of early Alzheimer's disease pathologic change: Implications for disease pathogenesis. *Alzheimers Dement* 15:93–105. <https://doi.org/10.1016/j.jalz.2018.06.3057>
  99. Jester HM, Gosrani SP, Ding H, Zhou X, Ko MC, Ma T (2022) Characterization of early Alzheimer's disease-like pathological alterations in non-human primates with aging: a pilot study. *J Alzheimers Dis* 88:957–970. <https://doi.org/10.3233/jad-215303>
  100. Zhang J, Chen B, Lu J, Wu Y, Wang S, Yao Z et al (2019) Brains of rhesus monkeys display A $\beta$  deposits and glial pathology while lacking A $\beta$  dimers and other Alzheimer's pathologies. *Aging Cell* 18:e12978. <https://doi.org/10.1111/accel.12978>
  101. Nakamura S, Nakayama H, Uetsuka K, Sasaki N, Uchida K, Goto N (1995) Senile plaques in an aged two-humped (*Bactrian*) camel (*Camelus bactrianus*). *Acta Neuropathol* 90:415–418. <https://doi.org/10.1007/bf00315016>
  102. Head E (2011) Neurobiology of the aging dog. *Age (Dordr)* 33:485–496. <https://doi.org/10.1007/s11357-010-9183-3>
  103. Head E (2013) A canine model of human aging and Alzheimer's disease. *Biochim Biophys Acta* 1832:1384–1389. <https://doi.org/10.1016/j.bbadis.2013.03.016>
  104. Chambers JK, Tokuda T, Uchida K, Ishii R, Tabe H, Takahashi E et al (2015) The domestic cat as a natural animal model of Alzheimer's disease. *Acta Neuropathol Commun* 3:78. <https://doi.org/10.1186/s40478-015-0258-3>
  105. Podlisny MB, Tolan DR, Selkoe DJ (1991) Homology of the amyloid beta protein precursor in monkey and human supports a primate model for beta amyloidosis in Alzheimer's disease. *Am J Pathol* 138:1423–1435
  106. Johnstone EM, Chaney MO, Norris FH, Pascual R, Little SP (1991) Conservation of the sequence of the Alzheimer's disease amyloid peptide in dog, polar bear and five other mammals by cross-species polymerase chain reaction analysis. *Brain Res Mol Brain Res* 10:299–305. [https://doi.org/10.1016/0169-328x\(91\)90088-f](https://doi.org/10.1016/0169-328x(91)90088-f)
  107. Braak H, Braak E, Strothjohann M (1994) Abnormally phosphorylated tau protein related to the formation of neurofibrillary tangles and neuropil threads in the cerebral cortex of sheep and goat. *Neurosci Lett* 171:1–4. [https://doi.org/10.1016/0304-3940\(94\)90589-4](https://doi.org/10.1016/0304-3940(94)90589-4)
  108. Nelson PT, Greenberg SG, Saper CB (1994) Neurofibrillary tangles in the cerebral cortex of sheep. *Neurosci Lett* 170:187–190. [https://doi.org/10.1016/0304-3940\(94\)90270-4](https://doi.org/10.1016/0304-3940(94)90270-4)
  109. Davies ES, Morphew RM, Cutress D, Morton AJ, McBride S (2022) Characterization of microtubule-associated protein tau isoforms and Alzheimer's disease-like pathology in normal sheep (*Ovis aries*): relevance to their potential as a model of Alzheimer's disease. *Cell Mol Life Sci* 79:560. <https://doi.org/10.1007/s00018-022-04572-z>
  110. Rosen RF, Farberg AS, Gearing M, Dooyema J, Long PM, Anderson DC et al (2008) Tauopathy with paired helical filaments in an aged chimpanzee. *J Comp Neurol* 509:259–270. <https://doi.org/10.1002/cne.21744>
  111. Colman RJ (2018) Non-human primates as a model for aging. *Biochim Biophys Acta Mol Basis Dis* 1864:2733–2741. <https://doi.org/10.1016/j.bbadis.2017.07.008>
  112. Chen X, Errangi B, Li L, Glasser MF, Westlye LT, Fjell AM et al (2013) Brain aging in humans, chimpanzees (*Pan troglodytes*), and rhesus macaques (*Macaca mulatta*): magnetic resonance imaging studies of macro- and microstructural changes. *Neurobiol Aging* 34:2248–2260. <https://doi.org/10.1016/j.neurobiolaging.2013.03.028>
  113. Krstic D, Knuesel I (2013) Deciphering the mechanism underlying late-onset Alzheimer disease. *Nat Rev Neurol* 9:25–34. <https://doi.org/10.1038/nrneurol.2012.236>
  114. Nazem A, Sankowski R, Bacher M, Al-Abed Y (2015) Rodent models of neuroinflammation for Alzheimer's disease. *J Neuroinflammation* 12:74. <https://doi.org/10.1186/s12974-015-0291-y>
  115. Fakhoury M (2018) Microglia and astrocytes in Alzheimer's disease: implications for therapy. *Curr Neuropharmacol* 16:508–518. <https://doi.org/10.2174/1570159x15666170720095240>
  116. Lopez-Rodriguez AB, Hennessy E, Murray CL, Nazmi A, Delaney HJ, Healy D et al (2021) Acute systemic inflammation exacerbates neuroinflammation in Alzheimer's disease: IL-1 $\beta$  drives amplified responses in primed astrocytes and neuronal network dysfunction. *Alzheimers Dement* 17:1735–1755. <https://doi.org/10.1002/alz.12341>
  117. Lecca D, Jung YJ, Scerba MT, Hwang I, Kim YK, Kim S et al (2022) Role of chronic neuroinflammation in neuroplasticity and cognitive function: a hypothesis. *Alzheimers Dement* 18:2327–2340. <https://doi.org/10.1002/alz.12610>
  118. Bao H, Cao J, Chen M, Chen M, Chen W, Chen X et al (2023) Biomarkers of aging. *Sci China Life Sci* 66:893–1066. <https://doi.org/10.1007/s11427-023-2305-0>

**Publisher's Note** Springer Nature remains neutral with regard to jurisdictional claims in published maps and institutional affiliations.

Springer Nature or its licensor (e.g. a society or other partner) holds exclusive rights to this article under a publishing agreement with the author(s) or other rightsholder(s); author self-archiving of the accepted manuscript version of this article is solely governed by the terms of such publishing agreement and applicable law.